

## Supporting Information

### **Energetically Autonomous, Wearable, and Multifunctional Sensor**

Hsing-Hua Hsieh<sup>1</sup>, Fang-Chi Hsu<sup>2,\*</sup> and Yang-Fang Chen<sup>1,\*</sup>

<sup>1</sup> Department of Physics, National Taiwan University, Taipei 106, Taiwan.

<sup>2</sup> Department of Materials Science and Engineering, National United University, Miaoli 360, Taiwan

\*corresponding author. Email: fangchi@nuu.edu.tw (F. C. Hsu); yfchen@phys.ntu.edu.tw (Y. F. Chen)

The supporting information includes:

Section 1. Fabrication procedure for the integrated device

Section 2. Morphology of PET/PDMS/Pt sensor after pre-straining at 1% elongation strain.

Section 3. Performance of PET/PDMS/Pt sensor.

Section 4. Performance of solar cell under 1 and 0.2 sun illumination

Figure S1. The schematic diagram of the fabrication process for the integrated device.

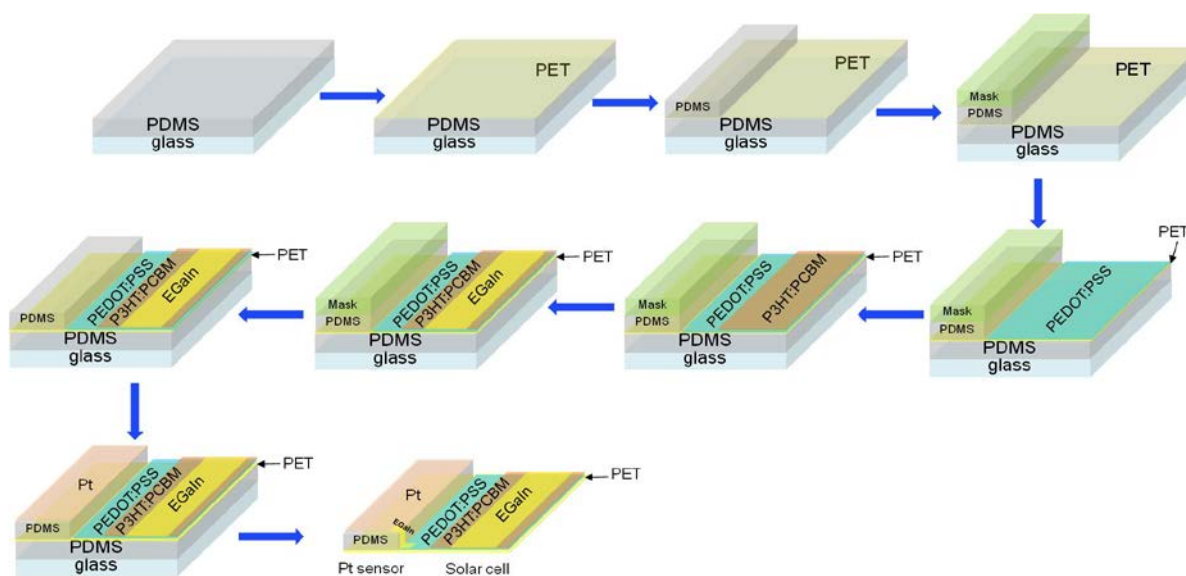
Figure S2. Morphology of PET/PDMS/Pt sensor. (a) The SEM image of the Pt film pre-strained at 1% elongation strain. (b) AFM image of PET/PDMS/Pt after pre-straining along with the surface profile analysis for locations 1,2,3, and 4 shown in (c).

Figure S3. The relative electrical resistance variation of the Pt film on PDMS under elongation and bending. (a) Selective I – V characteristics under various elongation strains from 0 to 2.0% strain with every 0.2% strain step. (b) Elongation mode. The corresponding GF values are summarized with data reading to the right axis. (c) Bending mode including extension and compression.

Figure S4. Performance of the stretchable solar cell. Current density ( $J$ ) – voltage ( $V$ ) characteristics of the stretchable solar cell under 1 and 0.02 sun AM 1.5G illumination. The schematic diagram for the device structure is shown in the inset

## Section 1. Fabrication procedures for the integrated device

Initially, a piece of rigid glass was used as the supporting substrate for the subsequent processing of soft polymeric materials such as PDMS, PET, PEDOT:PSS, and P3HT:PCBM to construct stretchable and flexible electrical and opto-electrical units on the same substrate. These two separate units were jointed through the application of EGaIn to bridge the Pt film of the sensor and the PEDOT:PSS electrode of the solar cell. Finally, the resulting integrated circuit, self-powered Pt strain sensor, was peeled off from the supporting glass through lifting up the soft PET layer, which became the new substrate afterwards.



**Figure S1.** The schematic diagram of the fabrication process for the integrated device.

## Section 2. Morphology of PET/PDMS/Pt strain sensor after pre-straining at 1% elongation strain

The as-prepared Pt film was continuous and exhibited no noticeable current change in response to the elongation strain below 1%. In regarding to this, the Pt film was pre-strained at 1% elongation strain to generate cracks on Pt surface. A gap of ~14 nm wide was developed for those cracks at 0% strain state as the SEM image shown in Figure S2a.

Figure S2b shows the AFM image of the Pt strain sensor after pre-strained. The waving feature is the characteristics of the PDMS layer after elongation. The orientation of cracks are either parallel or perpendicular to each other. The surface profile analysis for cracks located

1, 2, 3, and 4 are shown in Figure S2c. Among them, 1 and 2 are analyzed from crest to crest across the cracks while 3 and 4 are taken within troughs. The depth of those cracks is around 20 nm. The schematic of the Pt strain sensor is presented in (d).

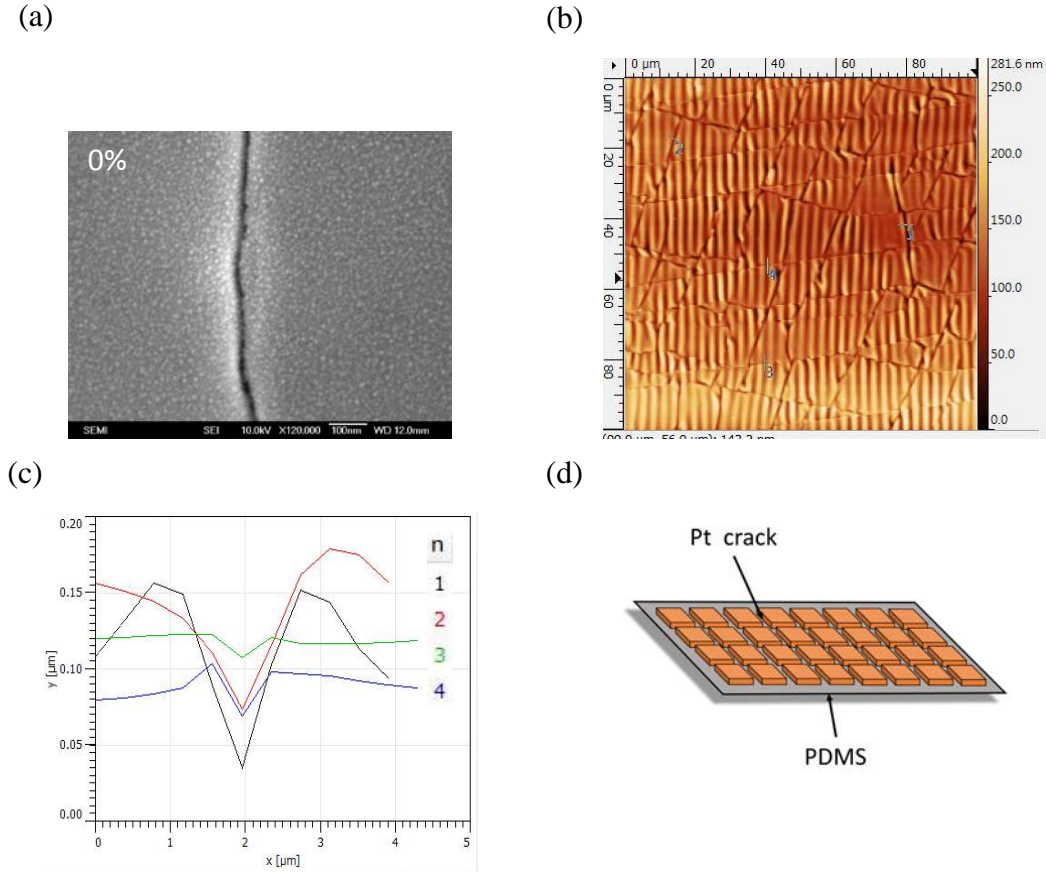


**Figure S2.** Morphology of PET/PDMS/Pt sensor. (a) The SEM image of the Pt film pre-strained at 1% elongation strain. The scale bar represents 100 nm. (b) AFM image of PET/PDMS/Pt after pre-straining along with the surface profile analysis for locations 1, 2, 3, and 4 shown in (c). (d) The schematic of the Pt strain sensor.

### Section 3. Performance of PET/PDMS/Pt strain sensor

Figure S3a shows the selective current–voltage (I–V) curves for the sensor under various elongation strain conditions. We calculated the corresponding resistance from each linear I–V curve and summarized the result in Figure S3b. Figure S3b characterizes the relative resistance variation ( $\Delta R/R_0$ ) of the PET/PDMS/Pt strain sensor after pre-strained under various elongation strains. The obtained elongation strain-dependent  $\Delta R/R_0$  relationship is reproducible within the strain range. Figure S3c illustrates  $\Delta R/R_0$  under bending motion,

leading to extension and compression of the sensor. The outward bending (extension) of the stretchable sensor results in an increase in resistance with bending radius whereas the reverse motion (compression) shows a decrease in the resistance.

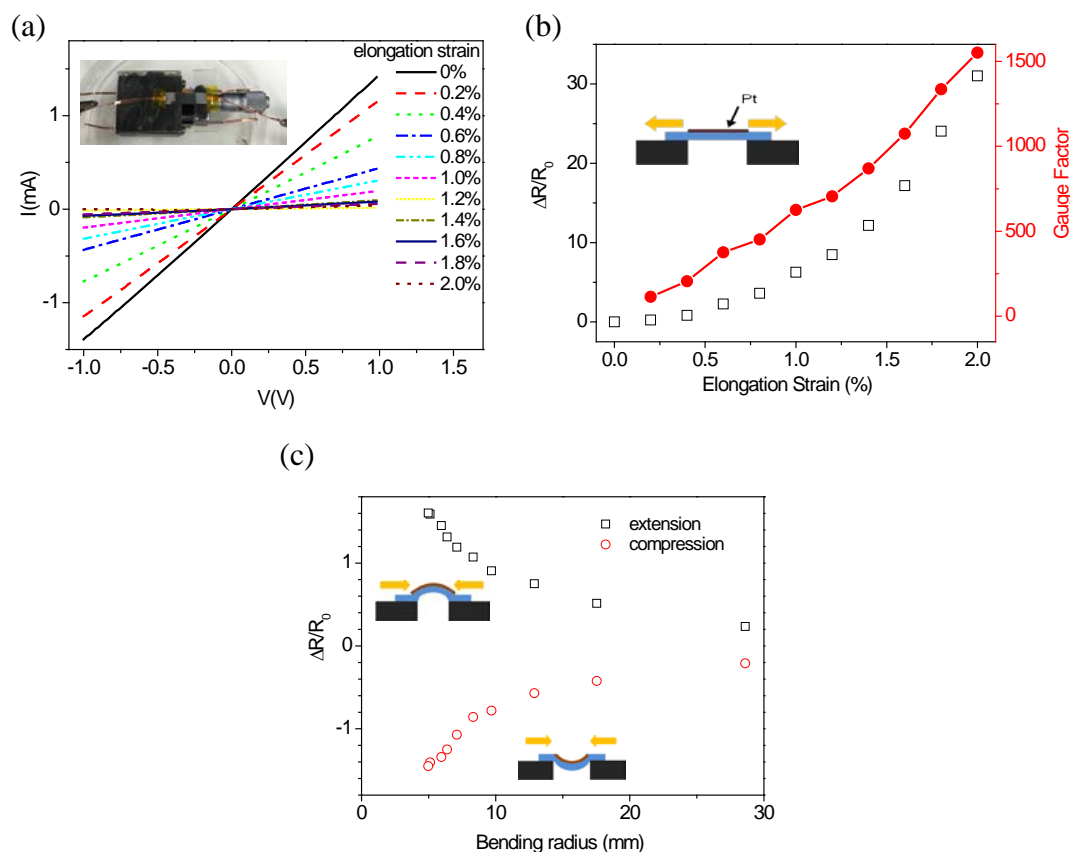


**Figure S3.** The relative electrical resistance variation of the Pt film on PDMS under elongation and bending. (a) Selective I – V characteristics under various elongation strains from 0 to 2.0% strain with every 0.2% strain step. The inset is the photograph for the measurement setup. (b) Elongation mode. The corresponding GF values are summarized with data reading to the right axis. (c) Bending mode including extension and compression.

#### Section 4. Performance of solar cell under 1 and 0.2 sun illumination

**Figure S4** depicts a typical current density–voltage ( $J$ – $V$ ) characteristic for fabricated PET/PEDOT:PSS/P3HT:PCBM/EGaIn solar cell before peeled-off from a glass substrate and the corresponding schematic diagram of the cell configuration is shown in the inset.

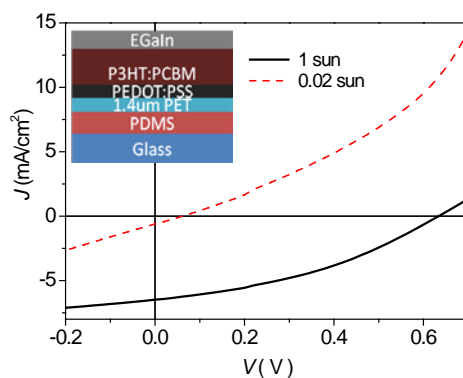


**Figure S4.** Performance of the stretchable solar cell. Current density ( $J$ ) – voltage ( $V$ ) characteristics of the stretchable solar cell under 1 and 0.02 sun AM 1.5G illumination. The schematic diagram for the device structure is shown in the inset